High-Pressure Melting of Molybdenum

A. B. Belonoshko,[1,2] S. I. Simak,[3] A. E. Kochetov,[3] B. Johansson,[1,3] L. Burakovsky,[4] and D. L. Preston[5]

[1]*Applied Materials Physics, Department of Material Science and Engineering, The Royal Institute of Technology, 10044 Stockholm, Sweden*

[2]*Condensed Matter Theory Group, The Royal Institute of Technology, 10691 Stockholm, Sweden*

[3]*Condensed Matter Theory Group, Department of Physics, Uppsala University, 75121 Uppsala, Sweden*

[4]*Theoretical Physics Divisions, Los Alamos National Laboratory, Los Alamos, New Mexico 87545, USA*

[5]*Applied Physics Divisions, Los Alamos National Laboratory, Los Alamos, New Mexico 87545, USA*

(Received 12 July 2003; published 13 May 2004)

The melting curve of the body-centered cubic (bcc) phase of Mo has been determined for a wide pressure range using both direct *ab initio* molecular dynamics simulations of melting as well as a phenomenological theory of melting. These two methods show very good agreement. The simulations are based on density functional theory within the generalized gradient approximation. Our calculated equation of state of bcc Mo is in excellent agreement with experimental data. However, our melting curve is substantially higher than the one determined in diamond anvil cell experiments up to a pressure of 100 GPa. An explanation is suggested for this discrepancy.

DOI: 10.1103/PhysRevLett.92.195701 PACS numbers: 64.70.Dv, 64.10.+h, 71.15.Pd

Properties of Mo have been extensively studied both experimentally [1–10] and theoretically [11–21]. Experimentally, it has been established that Mo is stable in a bcc structure up to the pressure (P) of at least 560 GPa at room temperature (T) [8], and that it melts at T of 2896 K at $P = 1$ bar [22]. Shock-wave measurements show that the Hugoniot first crosses a phase boundary at $P = 200$ GPa at an estimated $T = 4100$ K, and that it crosses a second phase boundary at $P = 372$ GPa at an estimated $T = 10\,000$ K [5]. Theoretical studies have been concerned primarily with Mo ground-state properties, apart from a few studies of high-P melting and solid-solid phase transitions [12,15]. Early papers [12,16] suggested that at $T = 0$ Mo is stable in the bcc structure up to $P = 3.1$ Mbar [12], where Mo transforms to a hexagonal close-packed (hcp) structure, and then at $P = 4.5$ Mbar to a face-centered close-packed (fcc) structure. Recent papers [18,19] suggest that at $T = 0$ the Mo hcp phase of Mo is not stable, and that bcc Mo transforms directly to the fcc phase at $P \gtrsim 7$ Mbar. Recently, Errandonea *et al.* [10] conducted the first diamond anvil cell (DAC) experiments to measure melting temperatures (T_m) of Mo to 100 GPa. The measured melting curve is in disagreement with shock-wave experiments [5,7]. While the DAC experiments showed that T_m varies from 2900 to 3100 K in the P interval 0–100 GPa, the T_m of Mo on the basis of shock-wave experiments was estimated to be around 10 000 K at $P = 372$ GPa. This dramatic difference requires an explanation.

Here we determine the melting curve of Mo over a wide range of P by (i) *ab initio* molecular dynamics (AIMD) simulations and (ii) a phenomenological theory of melting. Before carrying out the AIMD calculations of the melting curve, we first investigate their reliability by calculating Mo ground-state properties.

The calculations were done with the Vienna *ab initio* simulation package (VASP) [23,24]. Mo in the bcc, fcc, hcp, A15, and ω structures was studied in the framework of a full-potential frozen-core all-electron projected augmented wave method, with ionic relaxations taken into account. Semicore $3p$ states were treated as valence states. The energy cutoff was set to 224.6 eV. Exchange and correlation effects were treated in the framework of the generalized gradient approximation [25]. The integration over the Brillouin zone was done on special k points [26]. All necessary convergence tests were performed, and generally the required total energy convergence (0.2 mRy/atom) was reached for 20 to 770 k points in the irreducible wedge of the Brillouin zone, depending on the structure and total number of atoms.

The calculated $T = 0$ K Mo equation of state [Fig. 1(a)] is in very good agreement with experiment [6]. Mo is stable in the bcc structure at $T = 0$ up to 720 GPa where it transforms to the fcc phase [Fig. 1(b)]. This result is in perfect agreement with recent investigations [19].

Experimental data on the melting curve of Mo are rather scarce. There are two direct measurements of the Mo melting curve, the first to 9 GPa [2], and another to nearly 100 GPa (Fig. 2) [10]. The slope at the origin of the melting curve of Ref. [2], 8 K/GPa, does not agree with that obtained from isobaric-heating measurements of ΔH (enthalpy) and ΔV (volume) across the melting transition, 34 ± 6 K/GPa [3], though the uncertainties in Ref. [2] are large enough to accommodate the latter value for the slope.

We conducted our AIMD simulations in an NVE (N, number of particles; E, energy) ensemble at four volumes ($V = 15.48$, 12.19, 10.98, and 9.84 Å^3/atom) and $N = 128$ atoms arranged initially in an ideal bcc lattice. These volumes correspond to P of roughly 0, 1, 2, and

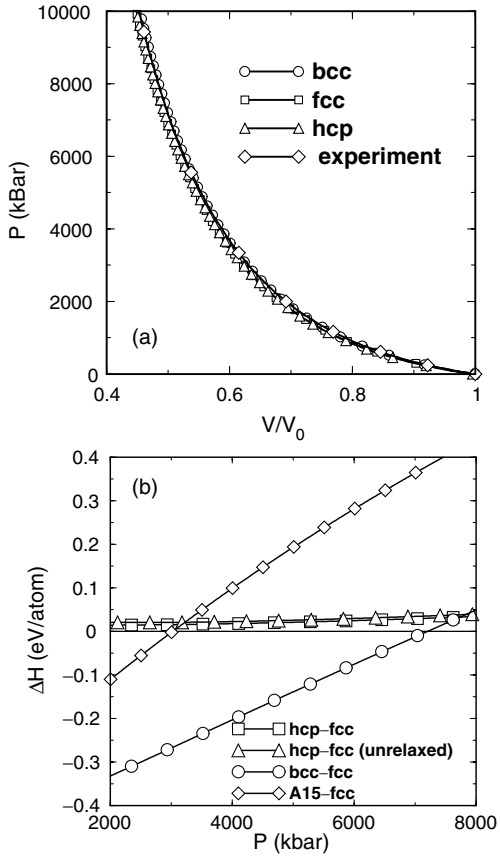

FIG. 1. (a) Calculated P as a function of compression of Mo phases compared to experiment [6] ($V_0^{\mathrm{exp}} = 15.576$, $V_0^{\mathrm{bcc}} = 16.192$, $V_0^{\mathrm{fcc}} = 16.190$, and $V_0^{\mathrm{hcp}} = 16.197\,\text{Å}^3/\text{atom}$). (b) Enthalpy differences as a function of P (negative sign means higher stability) between fcc and other phases of Mo as indicated in the legend.

3 Mbar at $T = 0$, respectively. At these volumes, we performed AIMD simulations at a number of T. We used a time step (τ) of 2 fs at the larger V and 1 fs at smaller volumes. One thousand τ was used for equilibration, during which velocities were scaled to the desired T every 5τ. Subsequently, the system evolved independently. With increasing T, we observed a discontinuous change of P, energy, and structure (Fig. 3). Close examination of the structural changes, as well as a dramatic increase in atomic mobility, confirmed that this discontinuous behavior is due to melting. The results of our AIMD simulations are presented in Fig. 2.

A theoretical melting curve of Mo can be constructed from the dislocation-mediated melting model [27–29]. In this theory, the dimensionless ratio

$$\chi(V_m) \equiv \frac{G(V_m, T_m(V_m))V_m}{k_B T_m(V_m)} \tag{1}$$

is a weak function of V_m, the solid V at melting. In what follows, we use density ρ rather than V; for Mo, $\rho = 1\ \mathrm{g\,cm^{-3}}$ corresponds to $V = 159.32\ \text{Å}^3/\text{atom}$. In Eq. (1) G is the shear modulus, which depends on both ρ and T. At fixed density, its T dependence is given in the Preston-

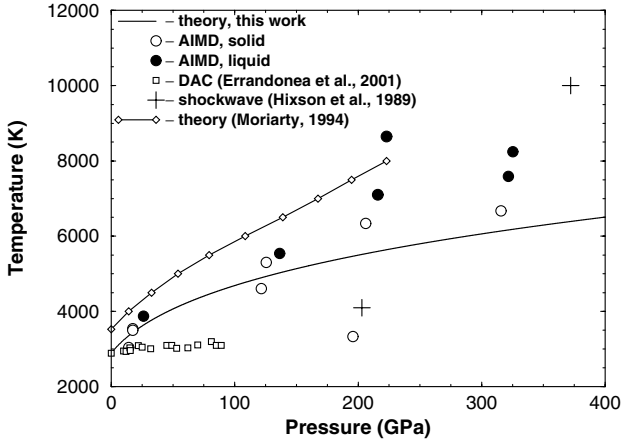

FIG. 2. Data and theory on the phases of Mo as a function of P and T. The solid curve is our theoretical melting curve for Mo [Eq. (4)]. Open circles indicate P and T at which Mo remained in the bcc phase during our AIMD runs, while solid circles indicate P and T where bcc Mo melted. Open squares are melting data obtained by the DAC technique [10]. The crosses are data from shock-wave experiments [5]. The cross at $P = 200$ GPa indicates a solid-solid transition, and the cross at $P = 372$ GPa corresponds to melting; the temperatures were estimated on the basis of theoretical calculations. The solid curve with diamonds is another theoretical prediction [12].

Wallace model [28] as

$$G(\rho, T) = G(\rho, 0)\left[1 - \beta\,\frac{T}{T_m(\rho)}\right]. \tag{2}$$

Here β is a constant, determined from $G(\rho_m, T_m(\rho_m)) = G(\rho_m, 0)(1 - \beta)$, where ρ_m is the melting point density at $P = 0$. We use the following values for Mo: $\rho_0 \equiv \rho(T = 0, P = 0) = 10.25\ \mathrm{g\,cm^{-3}}$, $\rho_m = \rho(T = T_m = 2896\,\mathrm{K}, P = 0) = 9.56\ \mathrm{g\,cm^{-3}}$ [22], $G(T = 0, P = 0) = 128.2$ GPa, and $G(T = T_m, P = 0) = 76.7$ GPa. The latter two values come from a very accurate fit to zero-P

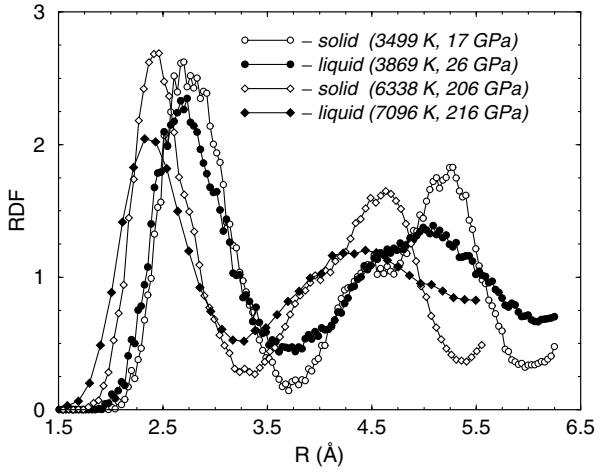

FIG. 3. Calculated radial distribution functions (RDF) of Mo at $V = 15.48\ \text{Å}^3/\text{atom}$ (circles) and $V = 10.98\ \text{Å}^3/\text{atom}$ (diamonds). Open symbols designate RDFs of bcc Mo and filled symbols designate liquid RDFs.

experimental data on G (to 1000 K) [1] of the form $G(T, P=0) = 128.2 - 1.86 \times 10^{-2} T \exp\{-128.8/T\}$. We also use the linear form $G(\rho, 0) = G(\rho_0, 0) + G'(\rho_0, 0) \times (\rho - \rho_0)$ with $G'(\rho_0, 0) = 40.5$ GPa/(g cm^{-3}), which very accurately describes the results of *ab initio* electronic structure calculations to a density $\sim$25 g cm^{-3} (compressions $\sim$2.5) [18]. This form gives $G(9.56\ \mathrm{g\,cm^{-3}}, 0) = 100.3$ GPa, and then, with $G(9.56\ \mathrm{g\,cm^{-3}}, 2896\ \mathrm{K}) = 76.7$ GPa, we find $\beta = 0.235$, close to the "canonical" value of 0.23 [28].

The value of χ at ρ_m is 32.0 for Mo. With increasing compression, χ must eventually approach a value of approximately 15 [29]. This value of χ is realized in the compression range 10^2 to 10^4 [30]. Hence $\chi(\rho)$ is indeed a very weak function of ρ as its value varies only by a factor of about 2 over 2–4 decades of compression. For Mo, we model $\chi(\rho)$ as a simple power form: $\chi(\rho) = 15 + 17\,(\rho_m/\rho)^q$, $q > 0$. Assuming that χ varies uniformly with density, i.e., by a factor of roughly 1.5 over 1–2 decades of compression, we obtain $0.2 \lesssim q \lesssim 0.4$, i.e., $q = 0.3 \pm 0.1$. With all the necessary ingredients in place, we finally obtain the theoretical Mo melting curve based on the dislocation-mediated melting model

$$T_m(\rho) = \frac{8837\,[128.2 + 40.5\,(\rho - 10.25)]}{\rho[15 + 17\,(9.56/\rho)^q]}, \qquad q = 0.3 \pm 0.1. \tag{3}$$

We expect this relation to be valid up to densities of at least 25 g cm^{-3} ($P \sim 11.5$ Mbar [18]), a range over which the use of a linear form for the Mo shear modulus is validated by [18].

The T_m as a function of P is now obtained by choosing the 21 density points from 9.5 to 19.5 (in g cm^{-3}) in increments of 0.5, and calculating the corresponding P based on T_m from Eq. (3) and the thermal equation of state of Mo from Ref. [31] (the highest density chosen, 19.5 g cm^{-3}, corresponds to $P = 9.7$ Mbar). The well-known Simon functional form $a\,(1 + bP)^c$ is then fit to the resulting 21 (P, T_m) points with the final result (P in GPa)

$$T_m(P) = 2896\left(1 + \frac{P}{18.6}\right)^{0.26}, \qquad 0 \le P \le 1000. \tag{4}$$

For Eq. (4), the slope at the origin is 40.5 K/GPa, consistent with Ref. [3]. This melting curve [Eq. (4)], along with the AIMD melting data, is shown in Fig. 2 and compared to previous data.

The discontinuous changes in Mo properties observed in our simulations occur at T higher than the theoretical T_m, a phenomenon known as overheating. The degree of overheating is rather small, about 10% of T_m at P around zero, and 15%–25% of T_m at higher P. This empirical observation is based on molecular dynamic (MD) simulations for a number of materials [32–35]. As a specific example, we carried out MD calculations of the overheating in iron with all simulation parameters (N, τ, equilibration time, etc.) exactly the same as for Mo. The volume was chosen to provide a P of about 3.7 Mbar; $P \le 3$ Mbar for the present study of Mo. By comparing to the T_m at this P [34], the overheating in Fe is estimated to be about 20%. Since overheating increases with P [32,33,35], we conclude that the overheating in Mo at 3 Mbar does not exceed 20%. This gives us very good agreement between our AIMD results and the theoretical melting curve (4). Overheating also depends on N. This dependence is rather strong at N below approximately 100, but quickly flattens at larger N [33]. Since $N = 128$ in our AIMD simulations, the size effect is small.

Normally, the difference between the heights of the first peaks of the solid and liquid radial distribution functions (RDFs) is nearly constant along the melting curve [36]. But from Fig. 3 we notice that this difference is substantially greater at higher P, because the height of the first peak of the liquid RDF at higher P is much lower than at lower P. This is typical for liquid RDFs calculated at T substantially higher than T_m. This implies that the overheating in our simulations increases with P, which is consistent with our experience [32–34]. We conclude that the T (7096 K) at which the high-P ($\sim$2 Mbar) liquid RDF was calculated is higher than the T_m. This conclusion is consistent with our theoretical melt curve (4) shown in Fig. 2.

The coordination number (CN) of a Mo atom at $T \lesssim T_m$ is equal to 14, which implies that in our AIMD simulations Mo melts from the bcc phase chosen initially. This does not necessarily mean, however, that the bcc phase of Mo is stable at high T. Our calculations indicate that the CN of liquid Mo is close to 12, which suggests that the liquid short-range order is similar to that of close-packed structures. Therefore, a close-packed solid phase might become stable at high T.

We now resolve the differences between our results on the melting and solid phase stability of Mo and the existing experimental data [5,7,10] and earlier theory [15]. The T_m estimated from the shock-wave experiment [5], namely, 10 000 K at a P of 372 GPa, is likely overestimated. This T_m is consistent with the theoretical melting curve of Ref. [15] (Fig. 2), which is already about 600 K higher than the experimental value (2896 K) at zero P. The T of the solid-solid phase transition at 2 Mbar (Fig. 2) is likely to be overestimated in the same proportion. This would bring the T of the solid-solid transition down from the 4100 K of Ref. [5] to around 3000 K. Note that this T is consistent with the DAC melting curve of Ref. [10].

While the shock-wave data [5,7] and theory [15] can be easily reconciled with our AIMD data (Fig. 2), the DAC melting curve [10] is considerably different. The DAC experiments [10] did not determine the structure of the emerging phase, and because of the close proximity of the T obtained by extrapolation of the DAC melting curve to 2 Mbar, namely, 3300 K, and the solid-solid transition T at 2 Mbar, around 3000 K, deduced from shock-wave data [5,7], we suggest that the DAC melting curve is in

fact a solid-solid phase boundary. The possibility of misinterpreting a solid-solid phase transition as melting [37] was recently demonstrated [38]. Our suggestion is also consistent with the tentative Mo phase diagram of Moriarty [12].

However, the structure of the emerging high-T solid phase remains unknown. We performed density-functional theory (DFT) calculations, trying to find possible solid-solid phase transitions in Mo at P and T in the range 2–10 Mbar and 300–6000 K. The goal was to check if the phase transition from bcc to fcc could be shifted to lower P by increasing T. The Helmholtz free energy was calculated from phonon frequencies. We have found that the P of the bcc to fcc transition increases with T. Therefore, we can exclude fcc as the high-T phase at a P of 2 Mbar. We have also performed NVE AIMD simulations of the A15 [12] phase at $V = 10.98$ Å^3/atom and $T = 6000$ K. We found that the A15 phase becomes unstable at this T and transforms to liquid. Since bcc Mo does not melt at the same V and T (Fig. 2), we conclude that the A15 phase is likely to be less stable than the bcc phase. Therefore, the solid-solid phase transition observed in shock-wave experiments [5] is not a bcc-fcc transition, and does not seem to be a bcc-A15 transition.

To conclude, we obtained T_m of the Mo bcc phase by DFT-based AIMD in the Born-Oppenheimer approximation. The temperatures are in good agreement with those obtained in the dislocation-mediated melting model [27]. The difference between the DAC data [10] and the melting curve in this work is alarming. Assuming that both the DAC technique and DFT are correctly applied, either the DAC technique based on the visual observation of an emerging phase leads to an erroneous conclusion or the AIMD method that we use fails. Since we do not see any clear reason why our method should fail, and since the structure of the emerging phase in the DAC experiments was not determined, we suggest that in the Mo DAC experiments of Ref. [10] a solid-solid transition was misinterpreted as melting. Experiments to determine the high-T structure must be carried out to resolve this issue.

L. B. wishes to thank S. D. Crockett and J. D. Johnson for stimulating discussions on the melting of Mo. J. A. Moriarty provided us with his Mo melting curve. Computations were performed using the facilities of the National Supercomputer Center in Linköping. Financial support from the Swedish Research Council and the Swedish Foundation for Strategic Research is acknowledged.

[1] J. M. Dickinson and P. E. Armstrong, J. Appl. Phys. **38**, 602 (1967); H. Wawra, Z. Metallkd. **69**, 518 (1978).
[2] N. S. Fateeva and L. F. Vereshchagin, Sov. Phys. JETP Lett. **14**, 153 (1971).
[3] J. M. Shaner, G. R. Gathers, and C. Minichino, High Temp. High Press. **9**, 331 (1977).
[4] A. C. Mitchell and W. J. Nellis, J. Appl. Phys. **52**, 3363 (1981).
[5] R. S. Hixson *et al.*, Phys. Rev. Lett. **62**, 637 (1989).
[6] Y. K. Vohra and A. L. Ruoff, Phys. Rev. B **42**, 8651 (1990).
[7] R. S. Hixson and J. N. Fritz, J. Appl. Phys. **71**, 1721 (1992).
[8] A. L. Ruoff, H. Xia, and Q. Xia, Rev. Sci. Instrum. **63**, 4342 (1992).
[9] P. Oelhafen, R. Wahrenberg, and H. Stupp, J. Phys. Condens. Matter **12**, A9 (2000); R. Wahrenberg *et al.*, Europhys. Lett. **49**, 782 (2000).
[10] D. Errandonea *et al.*, Phys. Rev. B **63**, 132104 (2001).
[11] B. K. Godwal and R. Jeanloz, Phys. Rev. B **41**, 7440 (1990).
[12] J. A. Moriarty, Phys. Rev. B **45**, 2004 (1992).
[13] N. Singh, Phys. Rev. B **46**, 90 (1992).
[14] S. M. Foiles, Phys. Rev. B **48**, 4287 (1993).
[15] J. A. Moriarty, Phys. Rev. B **49**, 12 431 (1994).
[16] P. Söderlind *et al.*, Phys. Rev. B **49**, 9365 (1994).
[17] G. Davidov, D. Fuks, and S. Dorfman, Phys. Rev. B **51**, 13 059 (1995).
[18] N. E. Christensen, A. L. Ruoff, and C. O. Rodriguez, Phys. Rev. B **52**, 9121 (1995).
[19] J. C. Boettger, J. Phys. Condens. Matter **11**, 3237 (1999).
[20] Y. Wang, D. Chen, and X. Zhang, Phys. Rev. Lett. **84**, 3220 (2000).
[21] E. A. Smirnova *et al.*, Phys. Rev. B **66**, 024110 (2002).
[22] D. C. Wallace, *Statistical Physics of Crystals and Liquids* (World Scientific, Singapore, 2002), p. 191.
[23] G. Kresse and J. Hafner, Phys. Rev. B **48**, 13 115 (1993).
[24] G. Kresse and J. Furthmüller, Comput. Mater. Sci. **6**, 15 (1996); Phys. Rev. B **54**, 11 169 (1996).
[25] Y. Wang and J. P. Perdew, Phys. Rev. B **44**, 13 298 (1991); J. P. Perdew *et al.*, Phys. Rev. B **46**, 6671 (1992).
[26] H. J. Monkhorst and J. D. Pack, Phys. Rev. B **13**, 5188 (1976).
[27] L. Burakovsky, D. L. Preston, and R. R. Silbar, Phys. Rev. B **61**, 15 011 (2000); J. Appl. Phys. **88**, 6294 (2000).
[28] D. L. Preston and D. C. Wallace, Solid State Commun. **81**, 277 (1992).
[29] L. Burakovsky, C. W. Greeff, and D. L. Preston, Phys. Rev. B **67**, 094107 (2003).
[30] N. N. Kalitkin and L. V. Kuzmina, Dokl. Phys. **47**, 778 (2002).
[31] Y. Zhao *et al.*, Phys. Rev. B **62**, 8766 (2000).
[32] A. B. Belonoshko, Geochim. Cosmochim. Acta **58**, 4039 (1994).
[33] A. B. Belonoshko *et al.*, Phys. Rev. B **61**, 3838 (2000); A. B. Belonoshko and L. S. Dubrovinsky, Am. Mineral. **81**, 303 (1996); A. B. Belonoshko, Phys. Chem. Miner. **25**, 138 (1998).
[34] A. B. Belonoshko, R. Ahuja, and B. Johansson, Phys. Rev. Lett. **84**, 3638 (2000).
[35] P. M. Agrawal, B. M. Rice, and D. L. Thompson, J. Chem. Phys. **118**, 9680 (2003); **119**, 9617 (2003).
[36] A. B. Belonoshko, High Press. Res. **10**, 583 (1992).
[37] R. Boehler *et al.*, Phys. Rev. Lett. **86**, 5731 (2001).
[38] A. B. Belonoshko, R. Ahuja, and B. Johansson, Phys. Rev. Lett. **87**, 165505 (2001); Nature (London) **424**, 1032 (2003); A. B. Belonoshko *et al.*, J. Chem. Phys. **117**, 7233 (2002).